

Unified Friction Formulation from Laminar to Fully Rough Turbulent Flow

Dejan Brkić^{1,*} and Pavel Praks^{1,2,*}

¹ European Commission, Joint Research Centre (JRC), Directorate C - Energy, Transport and Climate, Unit C3: Energy Security, Distribution and Markets, Via Enrico Fermi 2749, 21027 Ispra (VA), Italy

² IT4Innovations National Supercomputing Center, VŠB—Technical University of Ostrava, 17. listopadu 2172/15, 708 00 Ostrava, Czech Republic

* Correspondence: dejanbrkic0611@gmail.com, dejanrgf@tesla.rcub.bg.ac.rs (D.B.); Pavel.Praks@gmail.com, Pavel.Praks@ec.europa.eu (P.P.)

Abstract: This paper gives a new unified formula for the Newtonian fluids valid for all pipe flow regimes from laminar to the fully rough turbulent. It includes laminar, unstable sharp jump from laminar to turbulent, and all types of the turbulent regimes: smooth turbulent regime, partial non-fully developed turbulent and fully developed rough turbulent regime. The formula follows the inflectional form of curves as suggested in Nikuradse's experiment rather than monotonic shape proposed by Colebrook and White. The composition of the proposed unified formula consists of switching functions and of the interchangeable formulas for laminar, smooth turbulent and fully rough turbulent flow. The proposed switching functions provide a smooth and a computationally cheap transition among hydraulic regimes. Thus, the here presented formulation represents a coherent hydraulic model suitable for engineering use. The model is compared to existing literature models, and shows smooth and computationally cheap transitions among hydraulic regimes.

Keywords: Turbulent flow; Laminar flow; Pipes; Friction factor; Hydraulics; Monotonic roughness, Inflectional roughness; Smooth curve contact; Moody diagram; Hydraulic resistance.

1. Introduction

In hydraulics, resistance in pipe flow is represented usually through the Darcy flow friction factor λ which depends on the Reynolds number Re and the relative roughness of inner pipe surface ε [1]. All three quantities are dimensionless. For pipe flow, the Reynolds number Re usually takes values between 0 and 10^8 , while the relative roughness of inner pipe surface ε from 0 to 0.05. The relative roughness of inner pipe surface is not only characteristic of pipe material and its condition, but depends also on hydraulic flow regime ruled by the thickness of thin laminar boundary sub-layer of fluid near inner pipe surface [2,3] (Figure 1-up). In general, during pipe flow few different hydraulic regimes can occur (Figure 1); laminar (*a*), sharp transition from laminar to the smooth turbulent (*b*), smooth turbulent (c_1), non-fully developed partially turbulent (c_2) and fully developed rough turbulent (c_3):

(*a*): Absence of vortices is characteristic of laminar regime, while roughness of inner pipe surface does not have effect on flow,

(*b*) Transition for laminar to turbulent regime is sharp and almost immediate and can be described with sudden increase of the friction factor λ ,

(*c*) Higher values of the Reynolds number Re with vortices in flow are characteristic of turbulent regime: (c_1) First vortices in the middle of pipe are characteristic for the smooth turbulent regime, while still roughness of inner pipe surface is covered with laminar sub-layer, (c_2) With increase of the Reynolds number Re , thickness of the laminar sub-layer decreases and roughness of inner pipe surface starts to have important role, (c_3). In the case of fully rough turbulent flow, the roughness of inner pipe surface takes the dominant role.

Physical description of the different hydraulic regimes is given in Figure 1-up, while related diagrams in Figure 1-down.

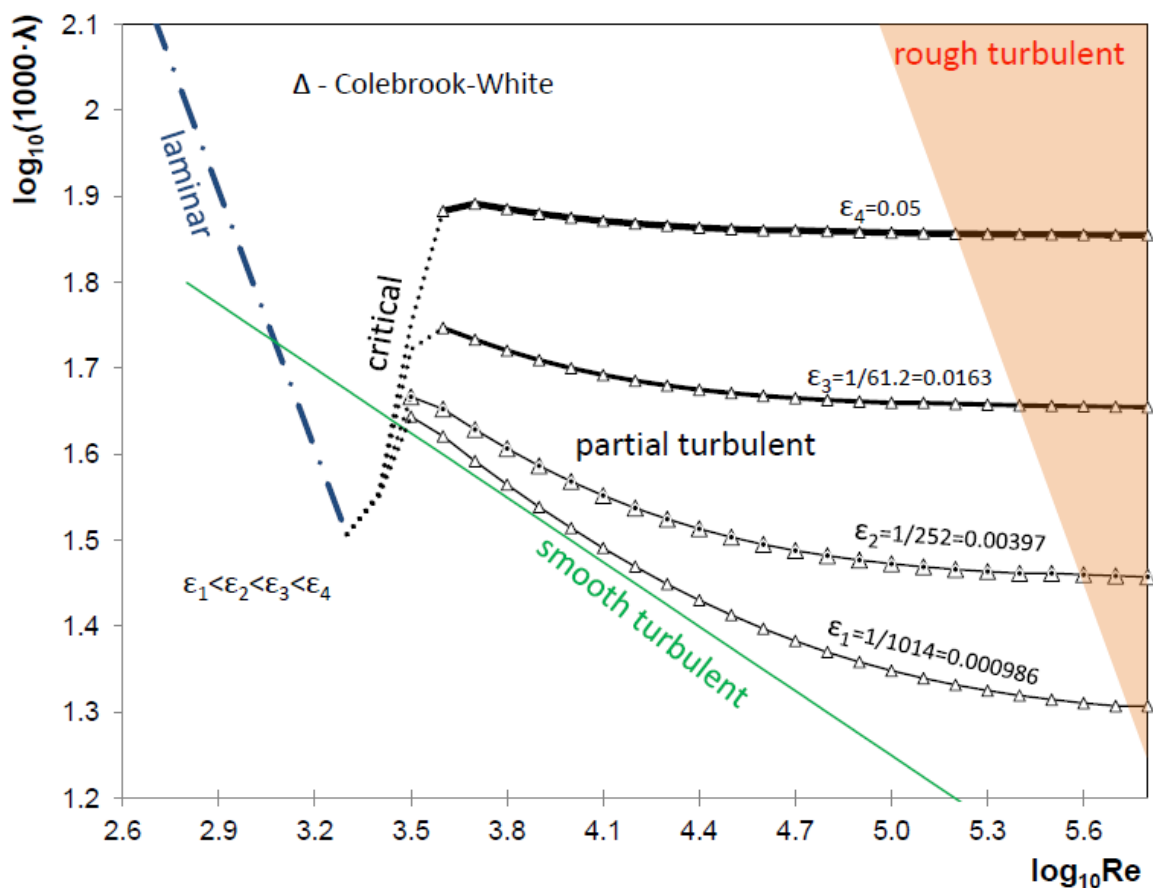
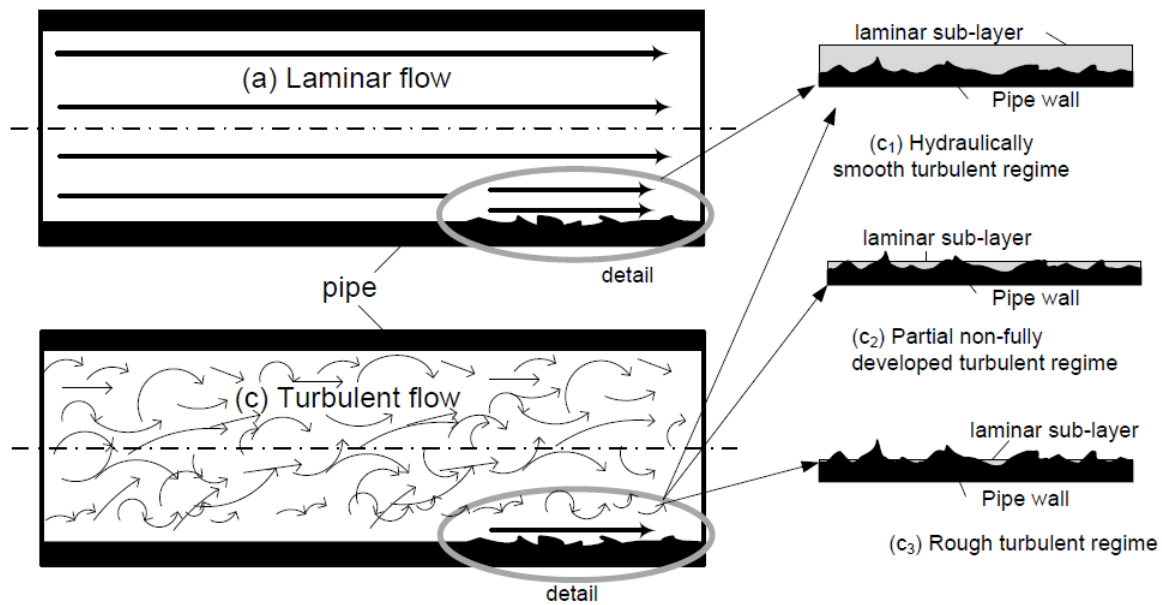


Figure 1. Hydraulic regimes for pipe flow: laminar (a), sharp transition from laminar to the smooth turbulent (critical) (b), smooth turbulent (c_1), non-fully developed partially turbulent (c_2) and fully developed rough turbulent (c_3); physical interpretation –up, and diagrams –down

Similar as Figure 1, the good representation of different hydraulic regimes gives widely known Moody diagram [4-6]. Turbulent part of the Moody diagram is based on the Colebrook equation [7].

While the formula for laminar regime; is very well theoretically founded, the formulas for all types of turbulent regimes are empirical [8-10]. Although coherent unified models for all hydraulic

regimes exist [11-13], they are not flexible as here presented because they are fixed (they do not allow changing separate formulas valid for different hydraulic regimes). In contrary, the here presented unified formula allows any of the formulas for the particular hydraulic regime to be included: one for laminar (a), one for hydraulically smooth turbulent (c_1) and one for fully developed rough turbulent (c_3). Thus, the here presented unified formula provides a smooth transition among hydraulic regimes using three switching functions y_1 , y_2 and y_3 ; see Eqs. (7-9) of this paper. The proposed unified formula is given by the following composition, Eq. (1):

$$\lambda = (1 - y_1) \cdot (a) + (y_1 - y_3) \cdot (c_1) + y_2 \cdot (c_3) \quad (1)$$

In Eq. (1), y_1 , y_2 and y_3 represent switching functions; a is a formula for laminar flow, $\lambda = \frac{64}{Re}$; while (c_1) is for smooth turbulent flow, $\lambda = \zeta(Re)$; and finally (c_3) is for fully developed rough turbulent flow, $\lambda = \zeta(\varepsilon)$. Here Re is the Reynolds number, ε is relative roughness of inner pipe surface while ζ and ς are functional symbols, respectively. Functions ζ and ς are empirical and related equations are available from literature [14].

The proposed unified formula follows the inflectional shape of curve as suggested in Nikuradse's experiment [8,15] rather than the monotonic shape of curves as proposed by Colebrook and White [7,9]. In our case, such shape is provided through carefully fitting of the switching functions y_1 , y_2 and y_3 . The Nikuradse's inflectional shape of curves is confirmed also by the recent Princeton and Oregon experiments with flow friction [14]. These two devices are significantly different but they reached similar conclusions; the Princeton facility uses compressed air, while Oregon uses helium, oxygen, nitrogen, carbon dioxide, and sulfur hexafluoride; the Princeton device weights approximately 25 tons, while the Oregon device weighs approximately 0.7 kg. Variant of the Moody diagram with included the Nikuradse's inflectional shape of curves also exists [16].

2. Previous works and source of their differences

Only few formulas valid for all hydraulic regimes exist; Eqs. (2-4), [11-13] respectively:

$$\lambda = 8 \cdot \sqrt[12]{\left(\frac{8}{Re}\right)^{12} + \left[\left(-2.457 \cdot \ln\left(\left(\frac{7}{Re}\right)^{0.9} + 0.27 \cdot \varepsilon\right)\right)^{16} + \left(\frac{37530}{Re}\right)^{16} \right]^{-1.5}} \quad (2)$$

$$\lambda = \sqrt[8]{\left(\frac{64}{Re}\right)^8 + 9.5 \cdot \left[\ln\left(\frac{\varepsilon}{3.7} + \frac{5.74}{Re^{0.9}}\right) - \left(\frac{2500}{Re}\right)^6 \right]^{-16}} \quad (3)$$

$$\lambda = 0.11 \cdot \sqrt[4]{\frac{\lambda_1 + \varepsilon + (28 \cdot \lambda_1)^{14}}{1 + 115 \cdot (28 \cdot \lambda_1)^{10}}} \quad (4)$$

$$\lambda_1 = \frac{68}{Re}$$

In Eqs. (2-4), λ is the Darcy friction factor, Re is the Reynolds number Re , and ε the relative roughness of inner pipe surface (all three quantities are dimensionless).

Turbulent part of Eqs. (2,3) are based on the Colebrook formula [7], while Eq. (4) is based on formulas from Russian engineering practice [17]. Turbulent part of Eq. (2) [11] is based on Churchill approximation of the Colebrook equation [18], while Eq. (3) [12] is based on Swamee and Jain approximation of the Colebrook equation [19]. As shown in Figure 2, the formulas from Russian practices and those based on the Colebrook equation give almost identical results for low values of relative roughness ε , while in the case of higher values of relative roughness ε , formulas from Russian practices give lower values for flow friction factor λ compared with the Colebrook equation. Both the Colebrook equation and formulas from Russian practice have monotonic shape of flow friction curves (Figure 2), which is disputed by some new experiments such as those from Princeton or Oregon laboratories [15], but also by an experiment of Nikuradse [8]. The experiment of

Nikuradse had been conducted in 1932 and 1933, while the experiment by Colebrook and White had been reported in 1937 [9]). The experiment of Nikuradse proposes a shape of curves in turbulent regime with an interval of declining values of friction factor λ before they reach their final maximal value for the fully developed rough turbulent flow. This property of flow friction is known as the Nikuradse's inflectional shape of transition to full turbulent regime (Figure 3) [20,21].

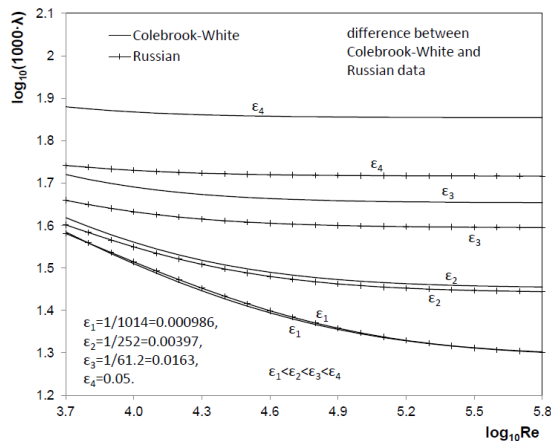


Figure 2. Different values of flow friction factor obtained using the Colebrook formula versus the formulas from Russian practice

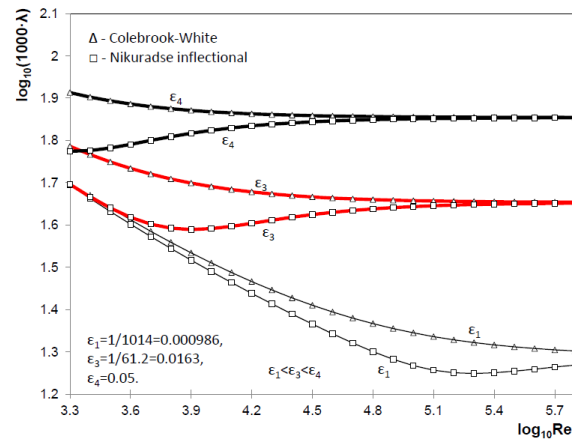


Figure 3. Different shapes flow friction factor curves obtained using the Colebrook formula versus those that follow Nikuradse's inflectional law

None of the currently available formulas valid for all hydraulic regimes; Eqs. (2-4), do not follow Nikuradse's inflectional law. The Colebrook equation can be extended to fit the data from Nikuradse's experiment; Eq. (5) [16]:

$$(c_2) \sim \frac{1}{\sqrt{\lambda}} = -2 \cdot \log_{10} \left(\frac{2.51}{Re} \cdot \frac{1}{\sqrt{\lambda}} + \frac{\varepsilon}{3.71} \cdot e^E \right) \quad (5)$$

$$E = \frac{-31.13}{Re \cdot \varepsilon} \cdot \frac{1}{\sqrt{\lambda}}$$

In Eq. (5), e is exponential function, where $E=0$ gives the Colebrook equation without Nikuradse's extension. The Colebrook equation is given in implicit form in respect to the flow friction factor λ [22-25], while the formulas from Russian practice is mostly belong to the explicitly given power-law type [26]. Anyway, as shown in Figure 4, the Colebrook equation is developed to unify in a smooth asymptotic way the von Karman-Prandtl equations for smooth turbulent flow and for fully rough flow; Eq. (6), but always having in mind that $\log(\alpha) + \log(\beta) \neq \log(\alpha + \beta)$:

$$(c_1) \sim \frac{1}{\sqrt{\lambda}} = 2 \cdot \log_{10}(Re \cdot \sqrt{\lambda}) - 0.8 = -2 \cdot \log_{10} \left(\frac{2.51}{Re} \cdot \frac{1}{\sqrt{\lambda}} \right) \quad (6)$$

$$(c_3) \sim \frac{1}{\sqrt{\lambda}} = 1.14 - 2 \cdot \log_{10}(\varepsilon) = -2 \cdot \log_{10} \left(\frac{\varepsilon}{3.71} \right) \quad \left. \right\} \rightarrow (c_2) \sim \frac{1}{\sqrt{\lambda}} = -2 \cdot \log_{10} \left(\frac{2.51}{Re} \cdot \frac{1}{\sqrt{\lambda}} + \frac{\varepsilon}{3.71} \right)$$

In Eq. (6), (c_1) presents smooth turbulent flow, (c_2) transitional non-fully developed turbulent flow and (c_3) fully developed rough turbulent flow. Similar strategies to unify and to modify the equation to conform to the certain laws (in our case Nikuradse's inflectional law) are used for our unified equation; see Eq. (1). On the other hand, Colebrook [9]; see Eqs. (5) and (6), uses logarithmic law to unify (c_1) and (c_3) in (c_2) . In our approach, we use switching functions y_1 , y_2 and y_3 to unify (a) , (c_1) and (c_3) in one coherent hydraulic model, where (a) represents laminar regime as already previously explained by Eq. (1).

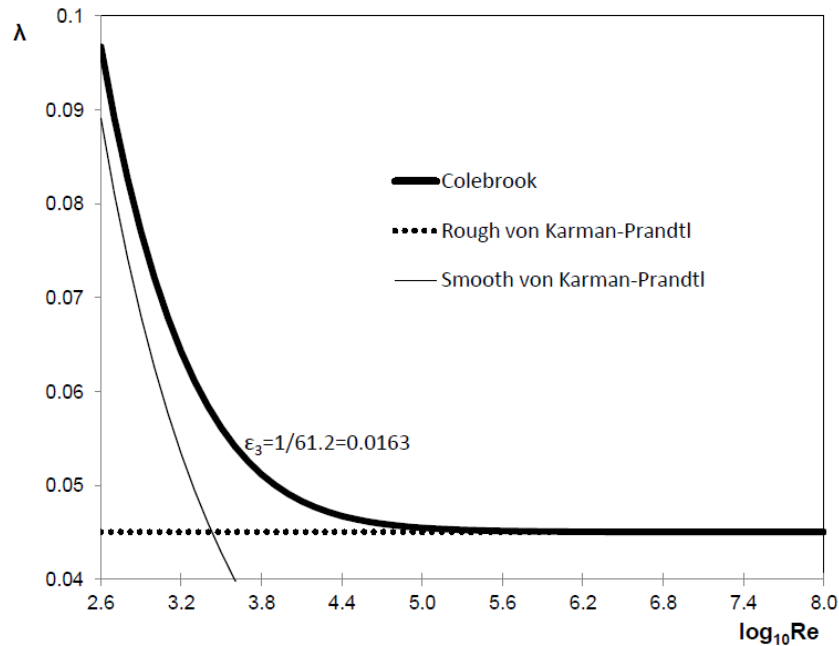


Figure 4. Von Karman-Prandtl equations for smooth turbulent flow and for fully rough flow unified by Colebrook using logarithmic function in one coherent hydraulic model

3. Switching functions, Friction factors, New formulation and Comparative analysis

Required inputs for the here presented unified formula; Eq. (1), are shown here: switching functions y_1 , y_2 and y_3 and formulas for friction factors for the certain hydraulic zones: (a)-laminar, (c_1)-smooth turbulent flow, and (c_3)-fully developed rough turbulent flow.

3.1. Switching functions

The unified formula valid for all hydraulic cases, in our case depends directly on switching functions y_1 , y_2 and y_3 . They provide smooth transition between different hydraulic regimes. Connection of curves provided using separate formulas for (a)-laminar, (c_1)-smooth turbulent flow, and (c_3)-fully developed rough turbulent flow, is not smooth without help of these three carefully selected switching functions y_1 , y_2 and y_3 . These three functions are rational, and they are generated in HeuristicLab, a software environment for heuristic and evolutionary algorithms [27]. The proposed switching functions have a simple form and therefore can be incorporated easily in computer codes without any significant burden of the Central Processing Unit [28]. The proposed switching functions y_1 , y_2 and y_3 are represented by Eqs. (7-9) and Figures 5-7, respectively.

$$y_1 = 1 - \frac{1048}{\frac{4.489}{10^{20}} \cdot Re^6 \cdot \left(0.148 \cdot Re - \frac{2.306 \cdot Re}{0.003133 \cdot Re + 9.646}\right) + 1050} \quad (7)$$

$$y_2 = 1.012 - \frac{1}{0.02521 \cdot Re \cdot \varepsilon + 2.202} \quad (8)$$

$$y_3 = 1 - \frac{1}{0.000389 \cdot Re^2 \cdot \varepsilon^2 + 0.0000239 \cdot Re + 1.61} \quad (9)$$

In Eqs. (7-9), symbols y_1 , y_2 and y_3 denote switching functions.

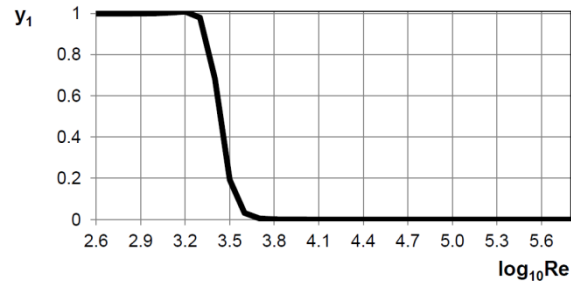


Figure 5. Switching function y_1 as a function of the Reynolds number with the main purpose to provide transition between (a)-laminar, (c₁)-smooth turbulent flow

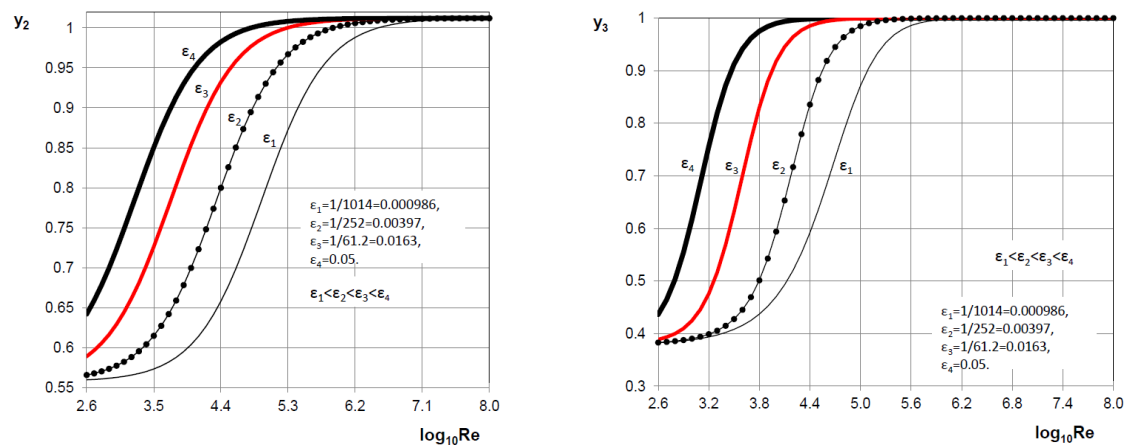


Figure 6. Switching function y_2 and y_3 with the main purpose to provide transition between (c₁)-smooth turbulent flow and (c₃)-fully developed rough turbulent flow

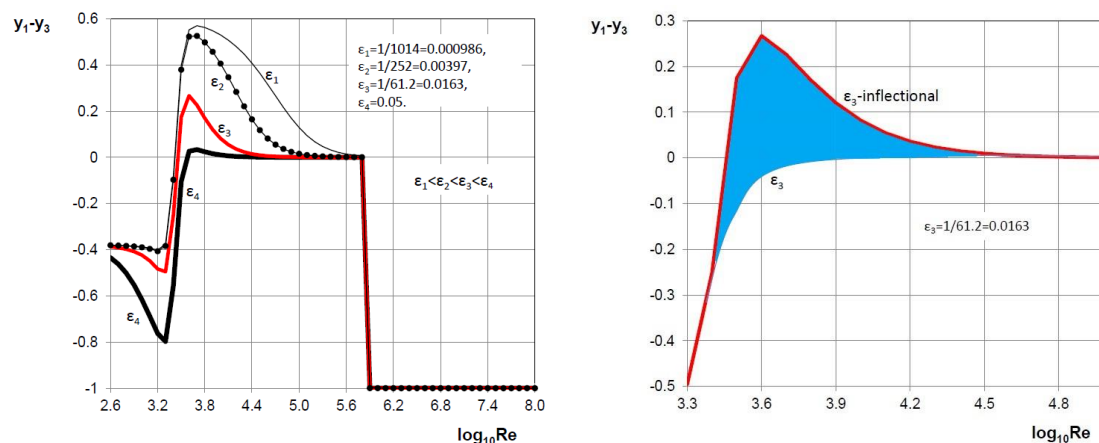


Figure 7. Function y_1-y_3 with the main purpose to provide Nikuradse's inflectional shape of the curves; on the right side: magnified detail from the left side – blue area presents the difference between Colebrook-White monotonic and Nikuradse's inflectional shape

3.2. Friction factors

Friction factors, which serve as inputs in the here presented unified formula, Eq. (1), will be here shown in more details; Here we present friction factors for (a)-laminar, (c₁)-smooth turbulent

flow, and (c_3)-fully developed rough turbulent flow hydraulic regimes. Turbulent flow is a phenomena that still causes a stir among experts [29,30]. Thus, the here shown relation is suitable for flow of Newtonian fluids, whereas some restrictions are applied for gases [31].

3.2.1. (a)-laminar

Due to the overriding effect of viscosity forces in laminar flow, even rough inner pipe surface appears to be hydraulically smooth for the Reynolds numbers lower than about 3000,. Consequently, the roughness of walls, unless it is very significant, does not affect the flow resistance. Under these conditions of the flow, the friction coefficient λ is always a function of the Reynolds number Re alone; Eq (10):

$$(a)\sim\lambda = \frac{64}{Re} \quad (10)$$

3.2.2. (c_1)-smooth turbulent flow

In the hydraulically smooth regime the friction factor, λ is a function of the Reynolds number Re only and the resistance to flow is independent of the relative roughness of inner pipe surface ε . This regime is restricted to the relatively small values of the Reynolds number Re where the roughness of inner pipe surface is completely hidden in the laminar boundary sub-layer. The literature on the hydraulically smooth regime abounds with reliable friction factor equations. In generally, with some extensions and modifications, there are Blasius form or power law relationships; Eq. (11)-up, and von Karman-Prandtl form or logarithmic relationships; Eq. (11)-down:

$$\left. \begin{aligned} (c_1)\sim\lambda &= A \cdot Re^{-B} \\ (c_1)\sim\frac{1}{\sqrt{\lambda}} &= C \cdot \log_{10}(Re \cdot \sqrt{\lambda}) - D \end{aligned} \right\} \quad (11)$$

Some possible values for coefficient A and exponent B for the Blasius form or power law relationships [17,26,31]; Eq. (11)-up, is given in Table 1:

Table 1. Power law relations for the hydraulically smooth turbulent regime

Equation in form: $\lambda=A \cdot Re^{-B}$	Coefficient A	Exponent B
Renouard	0.172	0.18
1/10 power law	0.139	0.18
modified 1/9 power law	0.184	0.2
1/9 power law	0.1748	0.2
1/8 power law	0.2252	0.22
1/7 power law	0.3052	0.25
Müller	0.3564	0.26
Blasius	0.3164	0.25
Panhandle A	0.08475	0.1461
Panhandle B	0.01471	0.03922
IGT (Institute of Gas Technology)	0.18086	0.19726
Towler and Pope	0.09458	0.15174
Mokhatab	0.02	0.185
Hodanovič	0.22	0.185

Regarding von Karman-Prandtl form or logarithmic relationships here is shown its basic form as used for a smooth part of the Colebrook equation, Eq. (12)-up. This formula is an updated version given by McKeon et al. [32], Eq. (12)-down:

$$\left. \begin{aligned} (c_1) \sim \frac{1}{\sqrt{\lambda}} &= 2 \cdot \log_{10}(Re \cdot \sqrt{\lambda}) - 0.8 = -2 \cdot \log_{10}\left(\frac{2.51}{Re} \cdot \frac{1}{\sqrt{\lambda}}\right) \\ (c_1) \sim \frac{1}{\sqrt{\lambda}} &= 1.884 \cdot \log_{10}(Re \cdot \sqrt{\lambda}) - 0.331 \end{aligned} \right\} \quad (12)$$

In addition, for the hydraulically smooth turbulent regime, among other, it is possible to use, Eq. (13), up to down: Genereaux, Leese, Nikuradse, Hermann, White and Konakov [17,26,31].

$$\left. \begin{aligned} (c_1) \sim \frac{1}{\sqrt{\lambda}} &= 1.6 \cdot \log_{10}\left(\frac{Re \cdot \sqrt{\lambda}}{2}\right) - 0.6 \\ (c_1) \sim \lambda &= 0.0072 + \frac{0.612}{Re^{0.35}} \\ (c_1) \sim \lambda &= 0.0032 + \frac{0.221}{Re^{0.237}} \\ (c_1) \sim \lambda &= 0.0054 + \frac{0.936}{Re^{0.3}} \\ (c_1) \sim \lambda &= \frac{1.02}{(\log_{10}(Re))^{2.5}} \\ (c_1) \sim \lambda &= \frac{1}{(1.81 \cdot \log_{10}(Re) - 1.5)^2} \end{aligned} \right\} \quad (13)$$

Though the Blasius forms or the power-law relationships, Eq. (11)-up, have the merit of simplicity, they also have certain disadvantages, one of which being that the relations can only be applied over a limited range of hydraulically smooth regime. Extrapolations beyond this range cannot be made with confidence. Figure 8 gives a comparison of some of the friction coefficients λ used in the hydraulically smooth turbulent regime. As can be seen, the friction factor λ corresponding to the Hodanovič equation has higher values than those for Panhandle B, see Table 1. This fact is a demonstration of how limited is the range of application of several of the available equations as many of them were developed for particular situations. For example, Panhandle B is valid for large-diameter pipelines, while Renoard is suitable for distribution PVC pipeline networks in urban areas. In addition, main constraint for using von Karman-Prandtl form or logarithmic relationships; Eq. (11)-down is its implicit form in respect of the flow friction λ .

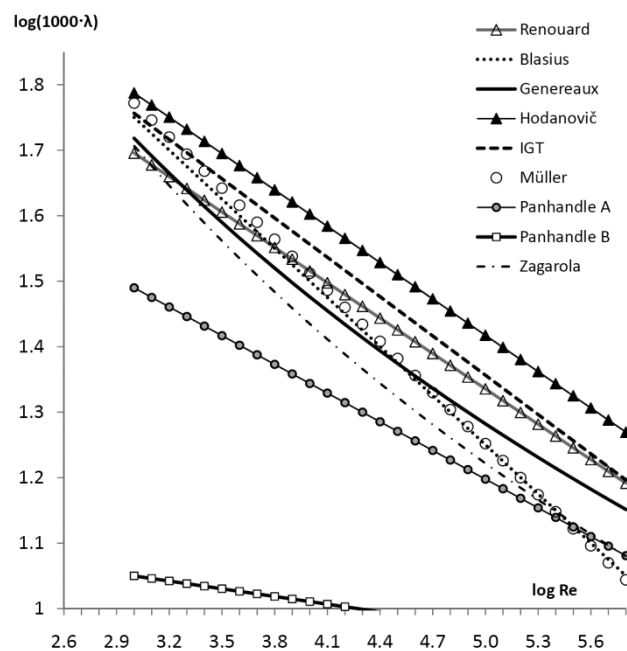


Figure 8. A comparison of some correlations for hydraulically smooth turbulent regime

3.2.3. (c_3) -fully developed rough turbulent flow

At high values of the Reynolds number Re , the friction factor λ becomes a constant for a given relative roughness ε [33]. In the case of the fully rough turbulent flow, the laminar sub-layer near the pipe wall practically does not exist and thus the flow is dominated by the relative roughness ε . The equation can be logarithmic; Eq. (14)-up, or power-law as used mostly in Russian engineering practice such as in so called Altshul or Shifrinson type of formulas; Eq. (14)-down [17]:

$$\left. \begin{aligned} (c_3) \sim \frac{1}{\sqrt{\lambda}} &= 1.14 - 2 \cdot \log_{10}(\varepsilon) = -2 \cdot \log_{10}\left(\frac{\varepsilon}{3.71}\right) \\ (c_3) \sim \lambda &= 0.11 \cdot \varepsilon^{0.25} \end{aligned} \right\} \quad (14)$$

A difference in results regarding Eq. (14) can be seen in Figure 2 of this paper.

3.3. New unified flow friction formulation

A novel formula for all hydraulic regimes is developed in order to easily encapsulate separate formulas for different hydraulic regimes into the one coherent hydraulic regime. The structure of the proposed formula, $\lambda = (1 - y_1) \cdot (a) + (y_1 - y_3) \cdot (c_1) + y_2 \cdot (c_3)$, is based on using three switching functions y_1 , y_2 and y_3 , and formulas for (a)-laminar, (c_1) -smooth turbulent flow, and (c_3) -fully developed rough turbulent flow. Consequently, all hydraulic regimes can be simulated in one simple formula including a sharp transition from laminar to the smooth turbulent (b) and non-fully developed partially turbulent regime (c_2). As already explained, the switching functions are set in such a way to produce always the Nikuradse's inflectional shape of the curves [34]. For example, two possible encapsulations in one unified coherent hydraulic model is given with Eq. (15) with the related diagrams in Figures 9 and 10, respectively.

$$\lambda = \left. \begin{aligned} &\frac{(a)}{Re} \cdot (1 - y_1) + \frac{(c_1)}{Re^{0.25}} \cdot (y_1 - y_3) + \frac{(c_3)}{\log_{10}^2\left(\frac{\varepsilon}{3.71}\right)} \cdot y_2 \\ &\frac{64}{Re} \cdot (1 - y_1) + \underbrace{\left(0.0032 + \frac{0.221}{Re^{0.237}}\right)}_{(c_1)} \cdot (y_1 - y_3) + \underbrace{0.11 \cdot \varepsilon^{0.25}}_{(c_3)} \cdot y_2 \end{aligned} \right\} \begin{array}{l} I \\ II \end{array} \quad (15)$$

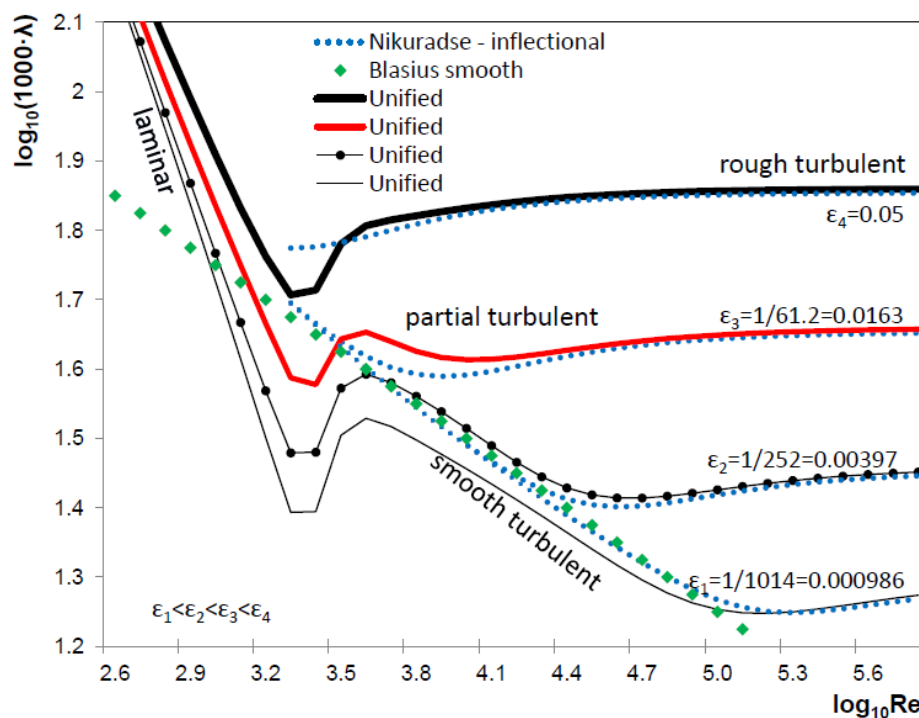


Figure 9. Unified hydraulic model I; Eq. (15)

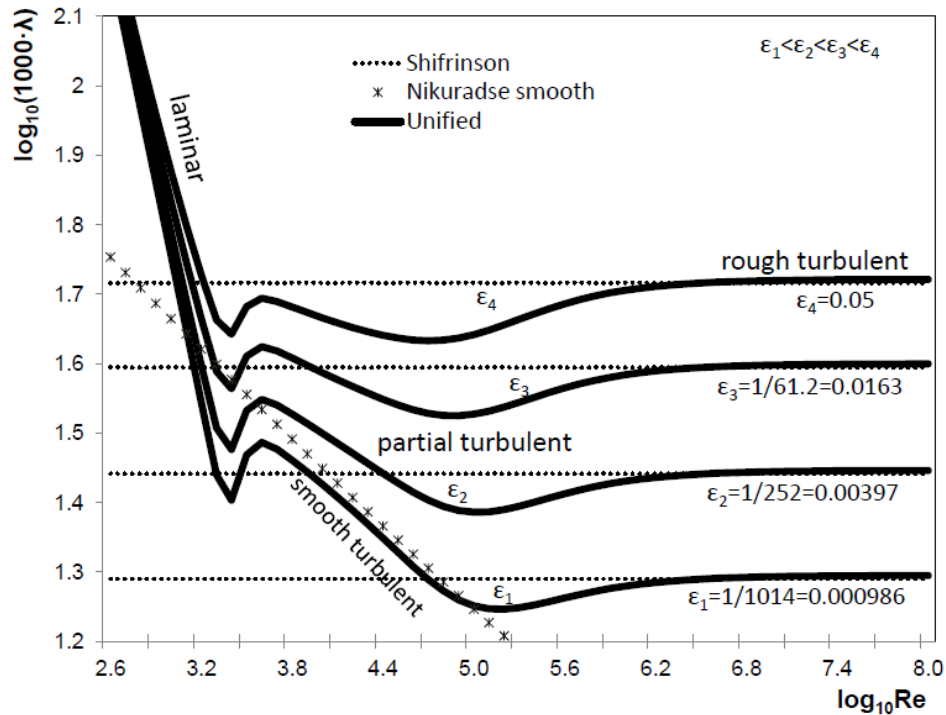


Figure 10. Unified hydraulic model II; Eq. (15)

In Figure 9, the blue dot-line shape is produced using the Colebrook equation with the extension for the Nikuradse's inflectional law; Eq. (5). Moreover, laminar flow (a) is given as usually by $\lambda = \frac{64}{Re}$, whereas the hydraulically smooth turbulent regime (c_1) with Blasius expression is represented as $\lambda = \frac{0.316}{Re^{0.25}}$. Finally, the fully developed turbulent regime (c_3) with von Karman-Prandtl equation $\lambda = \frac{0.25}{\log_{10}^2\left(\frac{\varepsilon}{3.71}\right)}$ is with the reference to Eq. (15)-I. For Figure 10, a similar approach is given by different formulas, as clearly indicated in Eq. (15)-II.

Using the same separate formulas for different hydraulic regimes from Eq. (15), one more additional encapsulation is possible, Eq. (16):

$$\lambda = \left. \begin{array}{l} \frac{(a)}{Re} \cdot (1 - y_1) + \frac{(c_1)}{Re^{0.25}} \cdot (y_1 - y_3) + \frac{(c_3)}{0.11 \cdot \varepsilon^{0.25}} \cdot y_2 \\ \frac{(a)}{Re} \cdot (1 - y_1) + \frac{(c_1)}{\left(0.0032 + \frac{0.221}{Re^{0.237}}\right)} \cdot (y_1 - y_3) + \frac{(c_3)}{\log_{10}^2\left(\frac{\varepsilon}{3.71}\right)} \cdot y_2 \end{array} \right\} \begin{array}{l} III \\ IV \end{array} \quad (16)$$

In such a way, after performing numerical tests, the most appropriate equation using separate available equations for different hydraulic can be encapsulated in a best way depending on particular circumstances required by each engineering project separately.

4. Conclusions

The paper presents new formula for a Newtonian fluids valid for all pipe flow regimes starting from laminar to the rough turbulent. Mentioned formula allows for the inflectional form what was presented in Nikuradse's experiment comparing to monotonic shape explained by Colebrook. The

composition consists of switching functions and interchangeable formulas for laminar, smooth turbulent and rough turbulent flow.

A sudden failure of valves or other components, either related to hydraulic systems in civil and mechanical engineering [35-37], can cause also change of flow regime. Because of that it is very important to take into consideration also such cases. The here presented unified flow friction approach is flexible, as proposed equations for certain hydraulic flow regime can be easily changed. Although our previous experiences with artificial intelligence [38-40] showed that encapsulation of all flow friction regimes into a one coherent model is not a straightforward task, the here proposed form is simple. Thus, the here presented unified approach can be easily implemented in software codes. Moreover, as the proposed switching functions are carefully chosen in such a way to follow the Nikurdse's inflectional law of roughness, the here proposed unified approach seems to be more realistic compared with the classical implicitly given 80 years old Colebrook-White monotonic curves model [41-43]. The here presented switching functions are expressed by a simple rational functions and thus do not contain computationally expensive transcendental functions. Consequently, the here presented unified flow friction formulation has also a reasonable computational complexity.

Author Contributions: The paper is a product of the joint efforts of the authors who worked together on models of natural gas distribution networks. P.P. has scientific background in applied mathematics and programming while D.B.'s background is in control and applied computing in mechanical and petroleum engineering. Based on the idea of D.B., P.P. used numerical data provided by D.B. to develop the presented switching functions in HeuristicLab [computer software]. D.B. prepared figures and wrote the draft of this article.

Conflicts of Interest: The authors declare no conflict of interest. Neither the European Commission, VŠB—Technical University of Ostrava nor any person acting on behalf of them is responsible for the use which might be made of this publication.

Nomenclature

The following symbols are used in this paper:

λ	Darcy friction factor (Moody, Darcy–Weisbach or Colebrook); dimensionless
Re	Reynolds number; dimensionless
ε	relative roughness of inner pipe surface; dimensionless
(a)	laminar
(c ₁)	smooth turbulent
(c ₂)	non-fully developed partially turbulent
(c ₃)	fully developed rough turbulent
y_1, y_2 and y_3 .	switching functions
e	exponential function
log	logarithmic function
ln	Napier natural logarithm
A, B, C, D and E	auxiliary terms

References

1. Brown, G.O. Henry Darcy and the making of a law. *Water Resources Research* **2002**, *38*, 11. <https://doi.org/10.1029/2001WR000727>
2. Brkić, D. Can pipes be actually really that smooth? *International Journal of Refrigeration* **2012**, *35*, 209-15. <https://doi.org/10.1016/j.ijrefrig.2011.09.012>

3. Shojaeizadeh, A.; Safaei, M.R.; Alrashed, A.A.; Ghodsian, M.; Geza, M.; Abbassi, M.A. Bed roughness effects on characteristics of turbulent confined wall jets. *Measurement* **2018**, *122*, 325-338. <https://doi.org/10.1016/j.measurement.2018.02.033>
4. Moody, L.F. Friction factors for pipe flow. *Transactions of the ASME* **1944**, *66*, 671-684.
5. LaViolette, M. On the history, science, and technology included in the Moody diagram. *Journal of Fluids Engineering* **2017**, *139*, 030801. <https://doi.org/10.1115/1.4035116>
6. Flack, K.A. Moving beyond Moody. *Journal of Fluid Mechanics* **2018**, *842*, <https://doi.org/10.1017/jfm.2018.154>
7. Colebrook, C.F. Turbulent flow in pipes with particular reference to the transition region between the smooth and rough pipe laws. *J. Inst. Civ. Eng.* **1939**, *11*, 133-156. <http://dx.doi.org/10.1680/ijoti.1939.13150>
8. Nikuradse, J. Laws of flow in rough pipes. Washington: National Advisory Committee for Aeronautics; 1950 (version in German from 1933: "Stromungsgesetze in rauhen Rohren"), available from: <http://ntrs.nasa.gov/archive/nasa/casi.ntrs.nasa.gov/199300939381993093938.pdf> (accessed on 15 September 2018)
9. Colebrook, C.; White, C. Experiments with fluid friction in roughened pipes. *Proc. R. Soc. Lond. Ser. A Math. Phys. Sci.* **1937**, *161*, 367-381. <http://dx.doi.org/10.1098/rspa.1937.0150>
10. Allen, J.J.; Shockling, M.A.; Kunkel, G.J.; Smits, A.J. Turbulent flow in smooth and rough pipes. *Philosophical Transactions of the Royal Society of London A: Mathematical, Physical and Engineering Sciences* **2007**, *365*, 699-714. <https://doi.org/10.1098/rsta.2006.1939>
11. Churchill, S.W. Friction-factor equation spans all fluid flow regimes. *Chem. Eng.* **1977**, *84*, 91-92.
12. Swamee, P.K. Design of a submarine oil pipeline. *J. Transp. Eng.* **1993**, *119*, 159-170. [https://doi.org/10.1061/\(ASCE\)0733-947X\(1993\)119:1\(159\)](https://doi.org/10.1061/(ASCE)0733-947X(1993)119:1(159))
13. Черников, В.А.; Черников, А.В. Обобщенная формула для расчета коэффициента гидравлического сопротивления магистральных трубопроводов для светлых нефтепродуктов и маловязких нефтей. *Наука и технологии трубопроводного транспорта нефти и нефтепродуктов* **2012**, *4*, 64-66. (in Russian), Available from: http://transenergostroy.ru/publications/src/20130424/Chernikin_gidrav_soprotivlenie.pdf (accessed on 15 September 2018)
14. Joseph, D.D.; Yang, B.H. Friction factor correlations for laminar, transition and turbulent flow in smooth pipes. *Physica D: Nonlinear Phenomena* **2010**, *239*, 1318-1328. <https://doi.org/10.1016/j.physd.2009.09.026>
15. Yang, B.H.; Joseph, D.D. Virtual Nikuradse. *Journal of Turbulence* **2009**, *10*, N11. <https://doi.org/10.1080/14685240902806491>
16. McGovern, J. Friction factor diagrams for pipe flow. 2011, Available from: <https://arrow.dit.ie/engschmecart/28/> (accessed on 15 September 2018)
17. Альтшуль, А.Д. Гидравлические Сопротивления; Недра: Moscow, Russia, 1982. (In Russian)
18. Churchill, S.W. Empirical expressions for the shear stress in turbulent flow in commercial pipe. *AIChE Journal* **1973**, *19*, 375-376. <https://doi.org/10.1002/aic.690190228>
19. Swamee, P.K.; Jain, A.K. Explicit equations for pipe flow problems. *J. Hydraul. Div. ASCE* **1976**, *102*, 657-664.
20. Sletfjerding, E.; Gudmundsson, J.S. Friction factor directly from roughness measurements. *Journal of Energy Resources Technology* **2003**, *125*, 126-130. <https://doi.org/10.1115/1.1576264>
21. Shockling, M.A., Allen, J.J., Smits, A.J. Roughness effects in turbulent pipe flow. *Journal of Fluid Mechanics* **2006**, *564*, 267-285. <https://doi.org/10.1017/S0022112006001467>
22. Brkić, D. Review of explicit approximations to the Colebrook relation for flow friction. *Journal of Petroleum Science and Engineering* **2011**, *77*, 34-48. <https://doi.org/10.1016/j.petrol.2011.02.006>
23. Praks, P., Brkić, D. Advanced iterative procedures for solving the implicit Colebrook equation for fluid flow friction. *Advances in Civil Engineering* **2018**, *2018*, 5451034. <https://doi.org/10.1155/2018/5451034>
24. Praks, P.; Brkić, D. Choosing the optimal multi-point iterative method for the Colebrook flow friction equation. *Processes* **2018**, *6*, 130. <https://doi.org/10.3390/pr6080130>
25. Praks, P.; Brkić, D. One-log call iterative solution of the Colebrook equation for flow friction based on Padé polynomials. *Energies* **2018**, *11*, 1825. <https://doi.org/10.3390/en11071825>
26. Brkić, D. A gas distribution network hydraulic problem from practice. *Petroleum Science and Technology* **2011**, *29*, 366-377. <https://doi.org/10.1080/10916460903394003>

27. Wagner, S.; Kronberger, G.; Beham, A.; Kommenda, M.; Scheibenpflug, A.; Pitzer, E.; Vonolfen, S.; Kofler, M.; Winkler, S.; Dorfer, V.; Affenzeller, M. Architecture and design of the HeuristicLab optimization environment, *Topics in Intelligent Engineering and Informatics* **2014**, *6*, 197–261. https://doi.org/10.1007/978-3-319-01436-4_10
28. Vatankhah, A.R. Approximate analytical solutions for the Colebrook equation. *J. Hydraul. Eng.* **2018**, *144*, 06018007. [https://doi.org/10.1061/\(ASCE\)HY.1943-7900.0001454](https://doi.org/10.1061/(ASCE)HY.1943-7900.0001454)
29. Cipra, B. A new theory of turbulence causes a stir among experts. *Science* **1996**, *272*, 951-951. <https://doi.org/10.1126/science.272.5264.951>
30. Chandrasekhar, S.; Sharma, V.M. Brownian heat transfer enhancement in the turbulent regime. *Facta Univ. Ser. Mech. Eng.* **2016**, *14*, 169–177. <https://doi.org/10.22190/FUME1602169C>
31. Bagajewicz, M.; Valtinson, G. Computation of natural gas pipeline hydraulics. *Industrial & Engineering Chemistry Research* **2014**, *53*, 10707-10720. <https://doi.org/10.1021/ie5004152>
32. McKeon, B.J.; Swanson, C.J.; Zagarola, M.V.; Donnelly, R.J.; Smits, A.J. Friction factors for smooth pipe flow. *Journal of Fluid Mechanics* **2004**, *511*, 41-44. <https://doi.org/10.1017/S0022112004009796>
33. Brkić, D. A note on explicit approximations to Colebrook's friction factor in rough pipes under highly turbulent cases. *International Journal of Heat and Mass Transfer* **2016**, *93*, 513-515. <https://doi.org/10.1016/j.ijheatmasstransfer.2015.08.109>
34. Thakkar, M.; Busse, A.; Sandham, N.D. Direct numerical simulation of turbulent channel flow over a surrogate for Nikuradse-type roughness. *Journal of Fluid Mechanics* **2018**, *837*, R1. <https://doi.org/10.1017/jfm.2017.873>
35. Nikolić, B.; Jovanović, M.; Milošević, M.; Milanović, S. Function k-as a link between fuel flow velocity and fuel pressure, depending on the type of fuel. *Facta Univ. Ser. Mech. Eng.* **2017**, *15*, 119-132. <https://doi.org/10.22190/FUME160628003N>
36. Praks, P.; Kopustinskas, V.; Masera, M. Monte-Carlo-based reliability and vulnerability assessment of a natural gas transmission system due to random network component failures. *Sustain. Resilient Infrastruct.* **2017**, *2*, 97–107. <https://doi.org/10.1080/23789689.2017.1294881>
37. Praks, P.; Kopustinskas, V.; Masera, M. Probabilistic modelling of security of supply in gas networks and evaluation of new infrastructure. *Reliab. Eng. Syst. Saf.* **2015**, *144*, 254–264. <https://doi.org/10.1016/j.res.2015.08.005>
38. Brkić, D.; Čojbašić, Ž. Intelligent flow friction estimation. *Comput. Intell. Neurosci.* **2016**, *2016*, 5242596. <http://dx.doi.org/10.1155/2016/5242596>
39. Brkić, D.; Čojbašić, Ž. Evolutionary optimization of Colebrook's turbulent flow friction approximations. *Fluids* **2017**, *2*, 15. <https://doi.org/10.3390/fluids2020015>
40. Praks, P.; Brkić, D. Symbolic regression-based genetic approximations of the Colebrook equation for flow friction. *Water* **2018**, *10*, 1175. <https://doi.org/10.3390/w10091175>
41. Uršič, M.; Kompore, B. Improvement of the hydraulic friction losses equations for flow under pressure in circular pipes. *Acta Hydrotechnica* **2003**, *21*, 57-74.
42. Bellos, V.; Nalbantis, I.; Tsakiris, G. Friction modeling of flood flow simulations. *J. Hydraul. Eng.* **2018**, *144*, 04018073. [https://doi.org/10.1061/\(ASCE\)HY.1943-7900.0001540](https://doi.org/10.1061/(ASCE)HY.1943-7900.0001540)
43. Cheng, N.S. Formulas for friction factor in transitional regions. *J. Hydraul. Eng.* **2008**, *134*, 1357–1362. [https://doi.org/10.1061/\(ASCE\)0733-9429\(2008\)134:9\(1357\)](https://doi.org/10.1061/(ASCE)0733-9429(2008)134:9(1357))